Investigation of the Size Control of Copper Ferrite Nanoparticles on their Electrical Properties in a Ferrofluid System using Oleic Acid Surfactant as an Energy Harvester

Ardan Rezon Prasetio[1,2], *Kimi* Alexander Lie[1,2], *Samuel* Jason Liwanto Lie[1,2], *Rosy* Eko Saputro[1,2], and *Willyanto* Anggono[1,3*]

[1]Centre for Sustainable Energy Studies, Petra Christian University, Surabaya, Indonesia
[2]SMA Kristen Petra 2, Surabaya, East Java, Indonesia
[3]Mechanical Engineering Department, Petra Christian University, Surabaya, East Java, Indonesia

Abstract. This research develops an energy harvesting system based on $CuFe_2O_4$ (copper ferrite) ferrofluid with size control using oleic acid as surfactant. The synthesis of copper ferrite nanoparticles as ferrofluid filler was carried out using the sonochemical method with the main iron source material being iron sand from Sine Beach, Tulungagung. Copper ferrite nanoparticles were coated with oleic acid in various volumes to control their size. After being completely coated, the mixture is dispersed in olive oil to become a complete ferrofluid. A series of characterizations was carried out comprehensively to confirm the success of this research, including characterization of structure, morphology, functional groups, and electrical properties. The structure of copper ferrite nanoparticles was identified using an X-ray diffractometry (XRD) instrument. It was discovered that the size of copper ferrite nanoparticles was 9.7 nm, and the structure formed was spinel reverse cubic with the highest peak of the HKL (3 1 1) plane located at an angle of 35.5°. The morphology of copper ferrite nanoparticles was observed via scanning electron microscope (SEM). Based on the results obtained, copper ferrite nanoparticles appear to agglomerate with particle clusters reaching 52 nm and an average particle size distribution of 25.1 nm. Functional group characterization was carried out using Fourier transform infrared (FTIR). The results showed that all precursors in the ferrofluid system had successfully emerged and formed. Analysis of electrical characteristics was carried out through I-V testing, and it was obtained that the CF3 sample with a volume of 3.6 mL of oleic acid had the highest current values of 13.1 μA, however, the three samples showed a good response and were representative for use as an energy harvester, which is promising.

1 Introduction

Electrical energy is a basic need for humans throughout the world. Until now, the need for electrical energy in every country has increased, including Indonesia. Reported from the Press Release of the Ministry of Energy and Mineral Resources of the Republic of Indonesia Number: 28.Pers/04/SJI/2024, electricity consumption by Indonesian citizens in 2023

increased to 1285 kWh/capita. In 2024, the Indonesian government is targeting an increase in electricity consumption per capita to reach 1408 kWh. Based on the press release, it can be concluded that the increase in electricity consumption per capita will definitely increase every year.

Unfortunately, this increase is not balanced with established innovations related to renewable energy sources. The reason is, the main electricity supply in Indonesia still uses fossil fuels, which are definitely decreasing in availability every year. Based on the above, researchers in Indonesia continue to strive for various innovations to obtain optimal electrical energy stability. In the last five years, Indonesian researchers have published many works related to renewable energy innovation, such as dye-sensitized solar cells (DSSC) [1], nano generators [2], water splitting [3], supercapacitors [4], and ferrofluid-based energy harvesters [5].

Related to ferrofluid-based energy harvesters, this method has the characteristic of converting external vibrations into electrical energy from an induced current [6]. The material used as the basis for this method is ferrofluid. This material is classified in the smart material category because of its ability to maintain a liquid-like phase even though it has been given a stimulus in the form of an external magnetic field [7]. The key to optimizing the ferrofluid-based energy harvesting method is the sloshing movement [7]. This movement dominantly influences the effectiveness of the ferrofluid in responding to an external magnetic field to produce magnetic flux [8].

Based on reference studies, in the last five years, this method has rarely been explored even though it has extraordinary renewable energy potential. Seeing prospective opportunities in developing this method, it is proposed to develop an energy harvesting method based on copper ferrite ferrofluid whose particle size is controlled through the use of surfactant. The use of this surfactant is necessary because the copper ferrite nanoparticles, which act as filler, have a tendency to agglomerate [9]. The next consideration is the stability factor. When not using surfactants, it will result in phase separation between the filler and dispersant, especially in long-term use [10].

Reviewing the two considerations above, in this study surfactant, namely oleic acid, was used. The choice of oleic acid as a surfactant is due to its ability to stabilize magnetic nanoparticles, thereby minimizing agglomeration tendencies in the ferrofluid filler and increasing its performance as an energy harvester [11]. Also, it is able to cover copper ferrite nanoparticles well and significantly contributes to the performance of ferrofluids [12].

2 Research Methods and Details

2.1 Materials

In this study the materials used consisted of iron sand, hydrochloric acid (HCl 12 M; 37%) from Merck, ammonium hydroxide (NH_4OH (6.7 M; 25%)) from Merck, cupric chloride ($CuCl_2$), alcohol (70%), oleic acid from Merck, olive oil and distilled water.

2.2 Synthesis of Copper Ferrite Nanoparticles

The synthesis carried out in this experiment followed the synthesis stages carried out and published by Saputro et al [13]. Natural sand taken from Sine beach, Tulungagung, was washed using distilled water, then dried in the sun. After the sand is dry, the sample is sieved to obtain really fine sand. The iron sand is then separated from the natural sand collection using a permanent magnet to obtain iron powder. Separation was carried out 15 times to remove impurities from the iron powder.

A total of 20 grams of iron powder resulting from the separation was reacted with 58 ml of HCl using a magnetic stirrer hotplate at a speed of 750 rpm at room temperature for 20 minutes. The result of this mixing is a solution of $FeCl_2$, $FeCl_3$, which is then filtered using filter paper. Next, 15 mL of $FeCl_2$, $FeCl_3$ solution was reacted with 1.04 grams of $CuCl_2$ and stirred with a magnetic stirrer at a speed of 550 rpm for 30 minutes at room temperature. Then, the mixture was titrated with 29 mL of NH_4OH via an ultrasonic bath with a frequency of 420 kHz while continuing to stir. The precipitate formed is copper ferrite nanoparticles and is then washed until pH = 7. A portion of the precursor is dried in an oven at 100 °C for 1 hour until it forms a powder for testing using XRD and SEM.

2.3 Synthesis of Copper Ferrite/Oleic Acid Ferrofluid

1 gram of copper ferrite precipitate was mixed with oleic acid varying in volume from 1 mL, 2 mL, and 3 mL in a magnetic stirrer hotplate with a speed of 750 rpm at a temperature of 90 °C for 1 hour. The use of temperature is intended to evaporate the water content in the sediment so that the oleic acid can properly cover the copper ferrite nanoparticles. Then the mixture was labelled as sample CF1, CF2, and CF3. Finally, the samples were dispersed in olive oil and ready for further characterization. The entire framework and stages of the synthesis are illustrated in Figure 1.

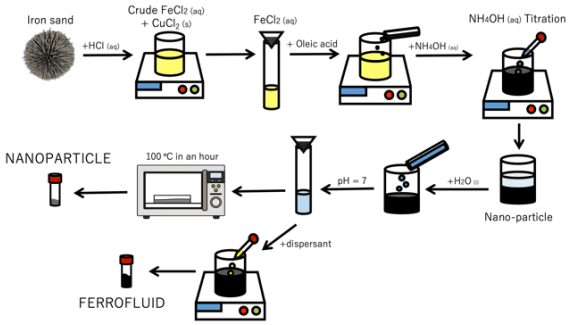

Fig. 1. Synthesis scheme for Copper Ferrite Nanoparticles and Ferrofluid

3 Results and Discussion

3.1 Structure Analysis of Copper Ferrite Nanoparticles

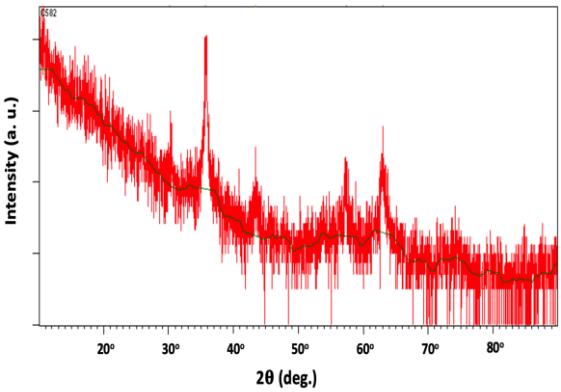

Fig. 2. X-ray diffraction pattern of copper ferrite

The XRD results of copper ferrite nanoparticles are shown in Figure 2. Based on the image, it can be seen that the peaks which representing magnetite phase appear at 30.1°; 35.6°; 43.2°; 57.2°; 62.6°, which corresponds to the Miller indices (2 2 0), (3 1 1), (4 0 0), (5 1 1), (4 4 0) [14]. The XRD data were fitted based on the AMCSD code database 0007423. The phase formed is entirely magnetite with a magnitude of lattice parameter $a = b = c = 8.350$ Å and has a crystal size of 9.7 nm. To strengthen the accuracy of particle size calculations, the Scherrer equation defined in equation 1 is also used.

$$D = \frac{K\lambda}{\beta \cos\theta} \quad (1)$$

D is the measured crystal size, K is a constant related to the crystal shape, generally having a value of 0.9, λ is the X-ray wavelength in nanometers, and β is the FWHM. Based on equation 1, a particle size of 9.5 nm is obtained. The results obtained have a difference of 0.2 nm and are still within the measurement tolerance threshold, so it can be claimed that the crystal size through refinement and the Scherrer equation agree. The results obtained indicate that coating using oleic acid has proven to be effective in controlling the particle size to become smaller. In a previous report, Nuñez et al. synthesized copper ferrite without using a surfactant obtained a larger crystal size, namely 12 nm [15].

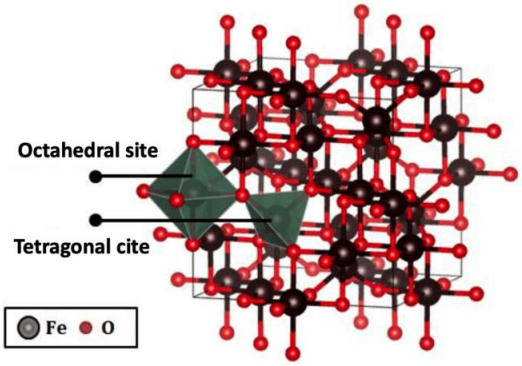

Fig. 3. Crystal visualization of copper ferrite

More deeply, theoretically, copper ferrite nanoparticles have a cubic inverse spinel structure as visualized in Figure 3. This has been fulfilled in this experiment by successfully showing the complete magnetite phase with a view of the diffracted characteristic peaks. Based on Figure 2, the oxygen and iron atoms that occupy the tetragonal and octahedral sites [16] are represented by black and red atoms, respectively. Furthermore, there are divalent cations at the tetragonal site and trivalent cations at the octahedral and tetragonal sites. Half of Fe^{3+} occupies tetragonal sites and all Fe^{2+} occupies octahedral sites with the general formulation $(Fe^{3+})\ [M_1{}^{2+}\ Fe^{3+}]O_4$ [17]. The characteristic features manifested by the atomic positions are what differentiate the copper ferrite crystal structure from the crystal structures of other iron derivative compounds [18].

3.2 Morphological Analysis of Copper Ferrite Nanoparticles

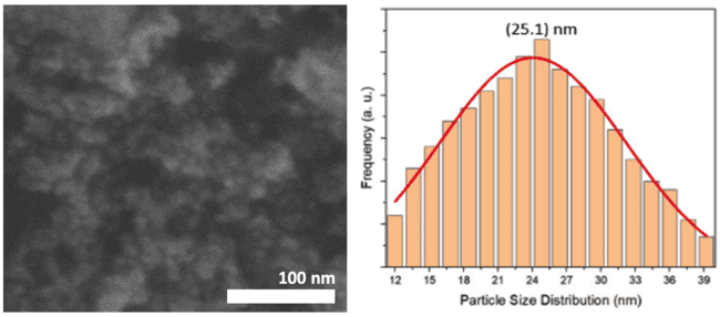

Fig. 4. SEM image and particle size distribution of copper ferrite nanoparticle

In this research, the morphology of the copper ferrite nanoparticles was identified through the scanning electron microscope (SEM) instrument. The morphology as well as the particle size distribution are shown in Figure 4. It was identified that the copper ferrite nanoparticles tended to agglomerate to form secondary particles or bigger clumps, which consist of primary particles. Generally, a high surface area-to-volume ratio naturally produces results in the form of van der Waals forces [19]. Therefore, the primary particles cluster to achieve a more stable state, which affects the formation of a single domain of copper ferrite nanoparticles [20]. Further analysis of the morphology of $CuFe_2O_4$ nanoparticles determined the particle size distribution [21]. This analysis was used as a reinforcement for structural analysis based on XRD data. The average particle size distribution of the samples is 25.1 nm.

However, the particle size distribution obtained showed relatively small values due to the influence of oleic acid as a surfactant. As a comparison, in research conducted by Lestari et al., they used plant extract-based surfactants and obtained a particle size distribution of up to 34.2 nm [22]. The next comparison is the use of polymer-based surfactants as done by Delianti et al., where they obtained particle size distribution values up to 39 nm [23].

3.3 Functional Groups Analysis of Copper Ferrite/Oleic Acid Ferrofluid

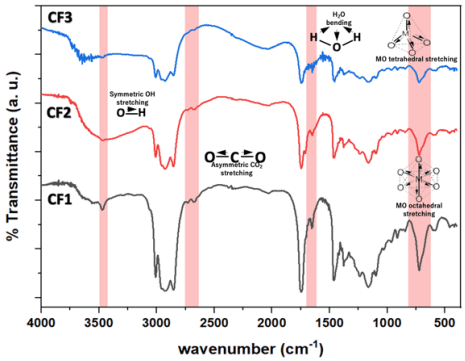

Fig. 5. FTIR spectra of copper ferrite/oleic acid ferrofluid

The functional groups of the three samples were characterized using FTIR, and the results shown in Figure 5 were obtained. This characterization was aimed at confirming the three components in the ferrofluid, namely: filler in the form of copper ferrite, surfactant in the form of oleic acid, and dispersing medium in the form of olive oil. M-O stretching bands in the 415 and 718 cm^{-1} areas represent the presence of metal bonds as filler in each sample [24].

Next, there are several stretching bands that characterize oleic acid, namely C=C in the 1311 and 1371 cm^{-1} area, COO- (carboxyl bond) in the 1467 cm^{-1} area, and CH_2 in the 2850 and 2922 cm^{-1} area [25-26]. Regarding the functional groups in oleic acid, it has non-polar hydrocarbon bonds and polar carboxylic acid bonds. This polar side will interact with the surface of the filler, and the non-polar side will interact with the dispersant in the ferrofluid, thereby making the filler hydrophobic and can be dispersed in organic solutions, thereby producing stable ferrofluids [27].

The next important component is the dispersion medium in the form of olive oil with several identified stretching bands, namely C-H in the 1094 cm-1 area, ester bonds (C-O) at 1170 and 1241 cm^{-1}, carbonyl esters at 1595 and 1744 cm^{-1} [28]. Furthermore, there are symmetric and asymmetric CH_2 bonds located in the area 2850 and 2922 cm^{-1}; these bonds are also shared by oleic acid, because olive oil has a high oleic acid content. Lastly, the typical bond that only olive oil has is the unsaturated bond, which appears in the 3007 cm^{-1} region [29]. With the appearance of filler functional groups, surfactant, and dispersing medium in the FTIR results, it can be well confirmed that copper ferrite/oleic acid ferrofluid has been successfully synthesized.

3.4 Electrical Properties Analysis of Copper Ferrite Ferrofluid

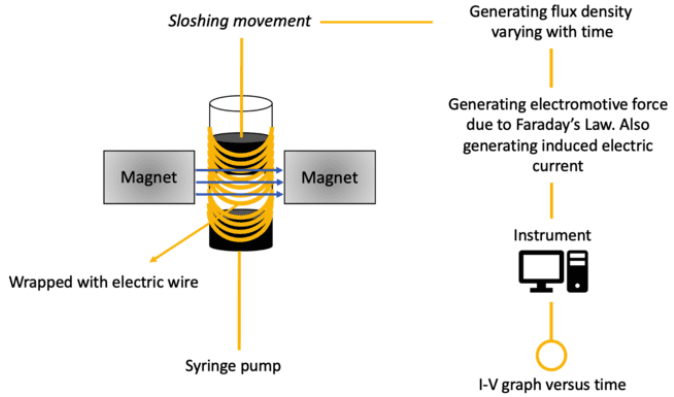

Fig. 6. I-V testing of copper ferrite ferrofluid

The measurement scheme of electrical quantities in the form of induced current and induced voltage is shown in Figure 6. Ferrofluid is pumped into a tube that has been wrapped in a current-carrying wire and is in an area with a magnetic field, as shown in the figure. This will cause the ferrofluid to experience sloshing movement, which then triggers the ferrofluid to appear to have a liquid-air-liquid pattern [30]. The consequence is that the formed liquid pattern acts as if it were an area that will be penetrated by a magnetic field. A magnetic field that penetrates a certain area is called magnetic flux. Furthermore, due to the sloshing movement in ferrofluid, the magnetic flux varies with time. Based on Faraday's law, when there is a magnetic flux that changes with time, it will produce an electromotive force [31]. In addition, based on this measurement, the induced electric current can also be known. The graphs of induced voltage and induced electric current from the measurements are shown in Figure 7.

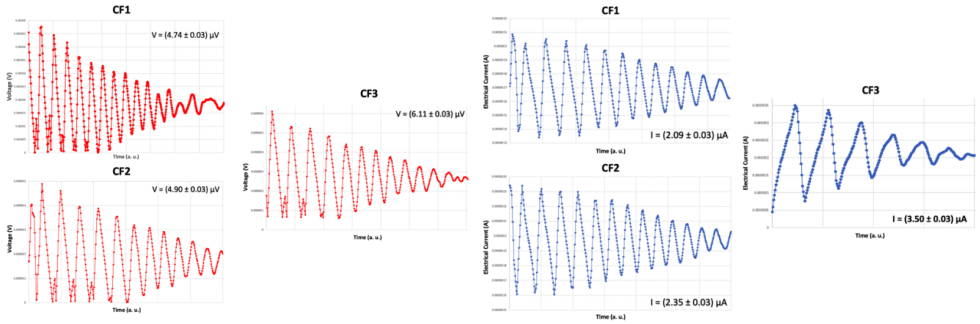

Fig. 7. (**red**)Voltage graph vs time of Copper Ferrite Ferrofluid, (**blue**)Electrical graph vs time of Copper Ferrite Ferrofluid

Based on Figure 7, it can be seen that the largest values of induced voltage and induced electric current are owned by the CF3 sample, which are 6.11 μV and 3.50 μA. Furthermore, the values of induced electric current and induced voltage can be used to determine electric power by multiplying the two quantities. The results of the calculation of electric power are shown in Table 1.

Table 1. Copper ferrite ferrofluid's electric quantities magnitude

Samples	Induced Electric Current (μA)	Induced Voltage (μV)	Electric power (pW)
CF1	2.09 ± 0.02	4.74 ± 0.02	9.91 ± 0.02
CF2	2.35 ± 0.02	4.90 ± 0.02	11.52 ± 0.02
CF3	3.50 ± 0.03	6.11 ± 0.03	21.39 ± 0.03

Referring to Table 1, along with the addition of oleic acid volume, the identified electrical magnitude also increased. This shows that the use of oleic acid as a surfactant has proven effective and successful in improving the electrical aspects of the sample [32]. Apart from that, the overall results of the sample show the potential of copper ferrite ferrofluid, which is promising for use as an energy harvester in the future.

4 Conclusion

Copper ferrite ferrofluid has been successfully synthesized from natural iron sand. Structural review identified the phase formed as magnetite with a lattice parameter value of 8.350 Å and a particle size of 9.7 nm. Morphological analysis showed agglomeration due to the tendency of nanoparticles to bond with each other, with a particle size distribution of 25.1 nm. The components of the ferrofluid, including filler, surfactant, and dispersant, were successfully revealed through the infrared spectrum. Measurement of electrical quantities, including induced voltage and induced electric current strength, showed potential as an energy harvester. The largest electrical quantity was possessed by the CF3 sample, which was the sample with the largest volume of oleic acid. This proves that the addition of oleic acid as a surfactant can improve the electrical properties of copper ferrite ferrofluid and can be prospective to become a new breakthrough in renewable energy devices.

References

1. A. Agrawal *et al.*, Solar Energy, **233,** (2022)
2. N. Mufti *et al.*, Mater. Sci. Energy Technol., **6**, (2023)
3. W. H. Saputera *et al.*, RSC Adv., **10**, 46 (2020)

4. M. Diantoro *et al.*, Int. J. Appl. Ceram. Technol., **20**, 4 (2023)
5. S. U. I. Subadra, A. Taufiq, "Ferrofluid $Mn_{0.5}Zn_{0.5}Fe_2O_4$ as Harvesting Energy: Preliminary Study," in *6th International Conference on Functional Materials Science*, (2023)
6. N. Hannon *et al.*, **14**, 8, (2023)
7. N. Anand, R. Gould, Fluids, **6**, 8, (2021).
8. L. Chen *et al.*, Int. J. Appl. Electromagn. Mech., **71**, 1, (2023)
9. P. M. Naullage *et al.*, ACS Cent. Sci., **5**, 3, (2019)
10. J. Kurimský *et al.*, J. Magn. Magn. Mater., **465**, (2018)
11. M. Vasilakaki *et al.*, Appl. Mater. Today, **19**, (2020)
12. M. Victory *et al.*, Mater. Chem. Phys., **240**, (2020)
13. R. E. Saputro *et al.*, Nano, **15**, 5, (2020)
14. M. Z. Sultan, *et al.*, J. Supercond. Nov. Magn., **34**, 12, (2021)
15. N. Nuñez *et al.*, Appl. Surf. Sci., **656**, (2024)
16. X. Zhang *et al.*, Inorg. Chem., **62**, 30, (2023)
17. T. K. H. Pham *et al.*, Journal of the Ceramic Society of Japan, **130**, 12, (2022)
18. K. V. Siva *et al.*, Mater. Sci. Eng. B, **284**, (2022)
19. E. G. Karvelas *et al.*, Comput. Methods Programs Biomed., **198**, (2021)
20. S. A. Al Kiey *et al.*, Appl. Phys. A, **128**, 6, (2022)
21. K. Cui *et al.*, Chin. J. Phys., **88**, (2024)
22. M. Lestari *et al.*, Mater. Today Proc., **44**, (2021)
23. D. Delianti, *et al.*, AIP Conf. Proc., **2687**, 1, (2023)
24. R. Jain, S. Gulati, Vibrational Spectroscopy, **126**, (2023)
25. F. S. Meibodi, E. Soori, J. Appl. Res. Water Wastewater, **10**, 1, (2023)
26. M. Nadeem *et al.*, Int. J. Nanoelectron. Mater. IJNeaM, **14**, 1, (2021)
27. M. S. Jagirani, M. Soylak, Turk. J. Chem., **45**, 6, (2021)
28. S. A. Ordoudi *et al.*, Molecules, **28**, (2023)
29. M. Cifuentes-Cabezas *et al.*, Chem. Eng. J., **454**, (2023)
30. B. Bao *et al.*, Energy Conversion and Management, **273**, (2022)
31. R. Maroofiazar, M. F. Farzam, Energy, **225**, (2021)
32. R. Maroofiazar, M. F. Farzam, Journal of Vibration Engineering & Technologies, **11**, (2023)